Armenian Journal of Physics, 2020, vol. 13, issue 3, pp. 228-234

Noise Reduction Methods in Laboratory of X-ray Microtomography

V.E. Asadchikov[1], A.V. Buzmakov[1], A.S. Ingacheva[1,2], Yu.S. Krivonosov[1], D.A. Zolotov[1], M.V. Chukalina[1,2,3]

[1]*Shubnikov Institute of Crystallography of Federal Scientific Research Centre "Crystallography and Photonics" of Russian Academy of Science, Leninskiy Prospekt 59, 119333, Moscow, Russia*
[2]*Institute for Information Transmission Problems RAS, Bolshoi karetnii per.9, 127051, Moscow, Russia*
[3]*Smart Engines, 60-letiya Oktyabrya Avenue, 9, 117312, Moscow, Russia*

E-mail: buzmakov@gmail.com

Received 22 June 2020

Abstract. Laboratory X-ray microtomography is a convenient method of studying the three-dimensional structure of objects of different types. Modern laboratory microtomography setups allow us to carry out measurements with submicron resolution. The laboratory sources of X-ray radiations used in such setups have low intensity, so the recorded tomographic projections are noisy. This often leads to the situation when the reconstructed tomographic images are also noisy, and artifacts may appear on them (objects of a characteristic shape, which are absent in the real object). In this work, we describe the methods of noise and artifacts suppression at all stages of data processing: reducing noise in the original projection images, the inclusion of regularizing members in the tomographic reconstruction procedure, filtering of reconstructed data. The reduction of noise and artifacts on tomographic data allows not only to reconstruct the internal structure of the objects under study but also to make a step towards temporal resolution and spectral tomography on laboratory sources.

Keywords: X-ray tomography, reconstruction, artifacts reduction

1. Introduction.

Laboratory $X-$ray microtomography [1] is used to study the three-dimensional structure of the objects in a nondestructive way. Modern microtomography setups allow us to carry out measurements with the resolution up to 1 nanometer [2, 3]. The spatial resolution of the tomographic method can be increased in various ways, for example, using a submicron probe in scanning schemes or applying optical schemes with magnification. However, an increase in spatial resolution inevitably leads to a decrease in the number of quanta collected by a detector cell per unit of time. At the same time, increasing the exposure time is not always possible, since the dose deposited in the sample increases proportionally. This can lead to degradation of the sample until its destruction. The conclusion suggests itself that it is necessary to develop the techniques for tomographic data handling that are able to work in conditions of a poor signal-to-noise ratio [4, 5]. In this work, we present the methods of noise and artifacts suppression in tomographic images at all stages of data processing: reducing noise in the original projection images, inclusion of regularizing members in the tomographic reconstruction procedure, filtering of reconstructed data.

2. How to work with tomographic projections.

Since all reconstruction methods are based on assumptions about the ideal hardware of the tomograph and the ideal implementation of the measurement scheme, any deviations from these assumptions introduce artifacts into the result of reconstruction. Let's describe the model of the experiment, which we use further to analyze the sources of error. The $X-$ray source and detector are stationary. The specimen under study is mounted on the holder. The sample holder is reinforced on the goniometer, allowing circular rotation of the sample with a given accuracy.

As was demonstrated [6] the source is not stable during the tomographic measurement. Measurement time can range from a few minutes to a few days. If the instability is not compensated, it can lead to slur (motion aberration) of different areas on the reconstructed image. The approach to correct the effect of thermal instability of the spot position is described [7].

Different detector cells have different quantum output. Miss calibration of the shells produces the rings on the reconstructed image (Fig. 1) due to vertical lines on the sinograms (Fig.2). In Fig.1 (left image) unfiltered sinogram was used to reconstruct the sample. Coaxial circles are well pronounced. There are different approaches to filter the lines. In [8] it was proposed to use one-dimensional low-pass filtering of the sums in Fourier space. The sum of all grey values of each column of a sinogram is calculated before the filtering. The filtering in sinogram space is evaluated in [9, 10].

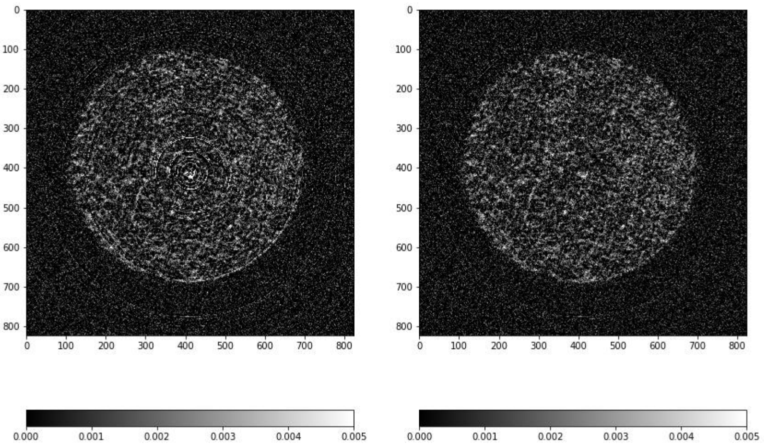

Fig.1. Left: Reconstruction without orthotropic artifacts removing. Right: Reconstruction after sinogram filtering.

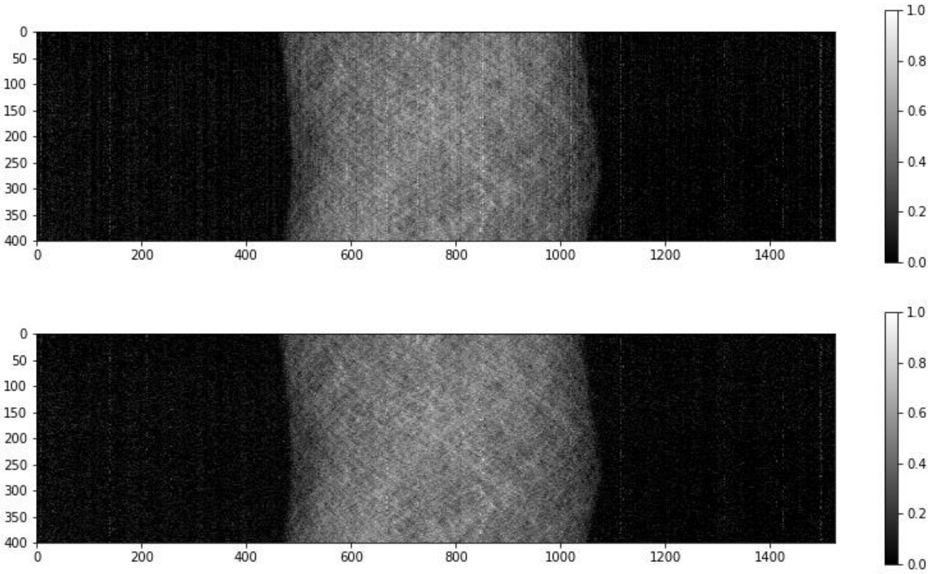

Fig.2. Up: Sinogram with orthotropic artifacts of image registration. Down: Result after filtering.

The tilt of the rotation axis, which causes by the measurement geometry, is the next problem. One of the approaches to solving the problem of 'aligning' geometry on the basis of the analysis of neighboring projections is presented in [11, 12].

3. Regularization-based reconstruction to reduce the noise influence

After all corrections of the measurement results (tomographic projections), they transfer to the reconstruction. There are different approaches to reconstruct the images. The most frequently, the integral approaches based on the inverse Radon transform are used. However, they produce not acceptable results in the presence of a high level of noise. To decrease the noise influence on the reconstruction result, the tomography inverse task is presented as a linear system of equations and it is solved by a non-linear optimization algorithm. In Fig.3 the result of the phantom reconstruction from the sinogram with high-level noise by algebraic approach is presented. To compare the reconstruction performed by different criteria, we present the cross-section of the phantom at the same Fig.3 on the right. Gray color corresponds to reconstruction by the algebraic method, and black one corresponds to Filtered Back Projection reconstruction.

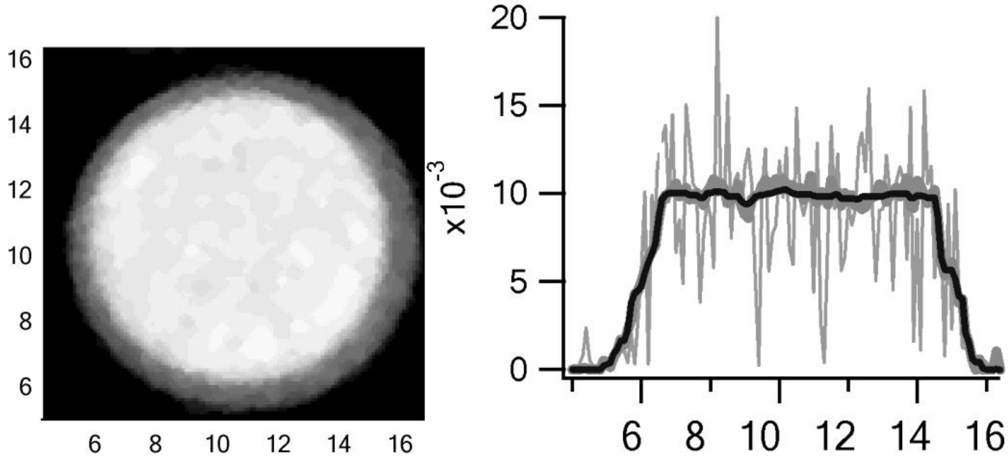

Fig. 3 Left: Reconstruction of the phantom from the sinogram with high-level noise. Right: Cross-section of the phantom.

The optimizing expression in the algebraic approach is a linear combination of two parts. The first one is a quadratic discrepancy in the tomographic projections space. The second term is a regularization part. In Fig.4 one tomographic projection of baby tooth with Pb inclusion inside from the set, collected in the "Crystallography and Photonics" Federal Researcher Centre of the Russian Academy of Science [13], is presented.

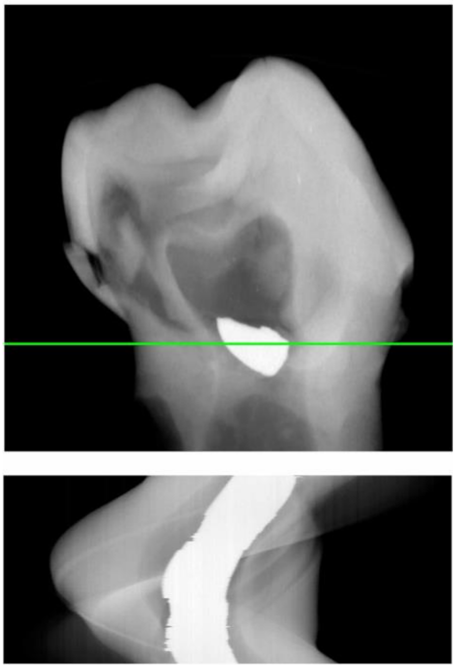

Fig.4 Tomographic projection and sinogram (corresponds to the green line on the projection) of the baby tooth.

An $X-$ray tube with Mo anode as a radiation source and a vacuum gauge for intensity stability reasons we used. The projections were collected with a XIMEA-xiRay 11 Mpix detector. The measurement parameters are - the tube was $40kV$ voltage, $20mA$ current and $5s$ acquisition time per frame. The object-source distance was $1.2m$ and the object-detector distance was $0.05m$. No filters were used. Every rotational scan consisted of 400 projections with an angular constant step size of $0.5\deg$. The detector pixel resolution was $9\,\mu m$. In Fig.5 we present the reconstruction of the cross-section from the sinogram presented in Fig 4. On the left the cross section reconstructed by the Filtered Back projection method is presented. Pb inclusion has very white border that does not correspond to the real case. The algebraic method was used to reconstruct the central and right images.

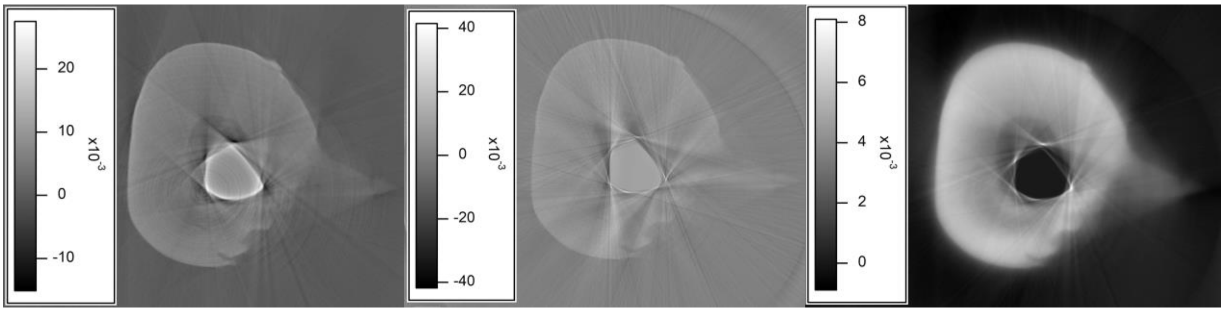

Fig.5 Cross-section reconstruction by FBP (left) and SIRT with different coefficients in linear combination.

4. Conclusions

We presented an overview of methods for noise suppression in tomographic reconstructions at all stages of data processing: noise reduction in the original projection images; usage the additional regularizing terms in the optimized expression on reconstruction step; filtering of reconstructed data. However, to suppress the noise completely is not possible. The filtering back-projection procedure applied to the image of the residual error built in the sinogram space will allow you to select the most dubious areas on the restored image [14]. It is a way to delegate to the end customers (for example, to the doctors) 2 images: final reconstruction result (like Fig. 6b) and the reconstruction from residual error (like Fig. 6b) as a criterion of the truthfulness of the reconstruction result.

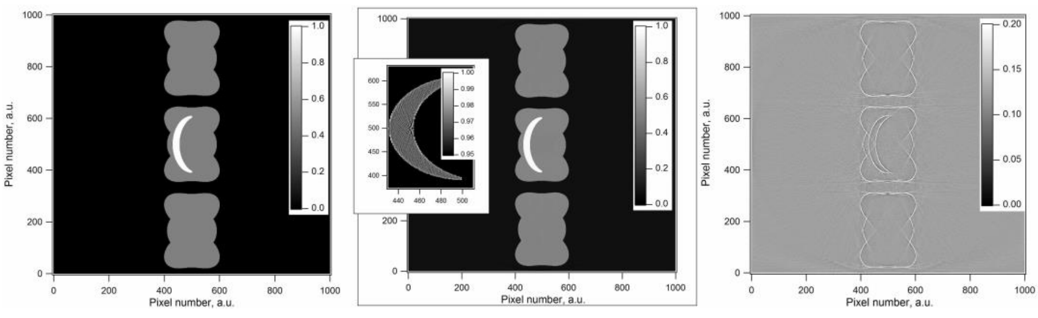

Fig.6 a - Phantom, b- reconstruction result, c- reconstruction from residual error.

The presence of an image containing the distribution of the remaining error reduces the odds of a wrong recognition decision [15] when a doctor diagnoses or rejects products formed during a multi-step manufacturing procedure. In the future we plan to include in our analysis the distortions [16] arises from optical elements added in optical gate to increase the registered image or to separate an individual energy line or a family of lines [17].

Funding

This work was supported by the Russian Foundation for Basic Research, project No. 19-01-00790 (reconstruction algorithms development) and project No. 17-29-03492 (tomography measurements) and by the Ministry of Science and Higher Education within the State assignment FSRC «Crystallography and Photonics» RAS (tomography reconstruction calculations)

Conflict of Interest

Authors have no conflicts of interests

Author Contributions

DZ, YK - obtain the experimental data; AI, MC – modeling and artifacts reduction; VA – discussion of the results; AB – tomography reconstruction; AB, MC, VA – participated in the writing of the text

References

[1] A. V. Buzmakov, V. E. Asadchikov, D. A. Zolotov, B. S. Roshchin, Yu. M. Dymshits, V. A. Shishkov, M. V. Chukalina, A. S. Ingacheva, D. E. Ichalova, Yu. S. Krivonosov, I. G. Dyachkova, M. Balzer, M. Castele, S. Chilingaryan, A. Kopmann. Laboratory Microtomographs: Design and Data Processing Algorithms. Crystallography Reports, Volume 63, Issue 6, pp 1057–1061, November 2018.

[2] Christopher T. G. Smith, Christopher A. Mills, Silvia Pani, Rhys Rhodes, Josh J. Bailey, Samuel J. Cooper, Tanveerkhan S. Pathan, Vlad Stolojan, Daniel J. L. Brett, Paul R. Shearingdand S. Ravi P. Silva. X-ray micro-computed tomography as a nondestructive tool for imaging the uptake of metalnanoparticles by graphene-based 3D carbonstructures. Nanoscale, Royal Society of Cemistry, 2019,11, 14734-14741, 19 Jul 2019.

[3] E. Longo, A. Bravin, F. Brun, I. Bukreeva, A. Cedola, O. De La Rochefoucauld, M. Fratini, X. Le Guevel, L. Massimi, L. Sancey, O. Tillement, P. Zeitoun. 3D imaging of theranostic nanoparticles in mice organs by means of x-ray phase contrast tomography. Proceedings Volume 10573, SPIE Medical Imaging 2018: Physics of Medical Imaging; 2018, 105734I.

[4] A. Buzmakov, V. Asadchikov, D. Zolotov, M. Chukalina Optimization of micro-tomographic experiment and reconstruction parameters at low signal-to-noise ratio. 12th Biennial Conference on High-Resolution X-Ray Diffraction and Imaging XTOP-2014. Villard-de-Lans, France. 2014. P.87.

[5] C. H. McCollough, L. Yu, J. M. Kofler, Sh. Leng, Yi Zhang, Zh. Li, R. E. Carter, Degradation of CT Low-Contrast Spatial Resolution Due to the Use of Iterative Reconstruction and Reduced Dose LevelsRadiology: Volume 276: Number 2—August 2015. P.499-506.

[6] A. Fukuda, K. Matsubara, I. Miyati T. Long-term stability of beam quality and output of conventional X-ray units. Radiol Phys Technol. 2015 Jan;8(1):26-9. doi: 10.1007/s12194-014-0282-1.

[7] A. S. Ingacheva, A. B. Buzmakov. Methods of Preprocessing Tomographic Images Taking into Account the Thermal Instability of the X-ray Tube. Optoelectronics, Instrumentation and Data Processing, March 2019, Volume 55, Issue 2, pp 138–147.

[8] M. Boin and A. Haibela. Compensation of ring artefacts in synchrotron tomographic images. Optics Express Vol. 14, Issue 25, pp. 12071-12075 (2006) •https://doi.org/10.1364/OE.14.012071.

[9] N.T. Vo, R. C. Atwood, M. Drakopoulos. Superior techniques for eliminating ring artifacts in X-ray micro-tomography. Optics Express Vol. 26, Issue 22, pp. 28396-28412 (2018) •https://doi.org/10.1364/OE.26.028396

[10] E.E. Berlovskaya, A.V. Buzmakov, A.S. Ingacheva, A.M. Makurenkov, D.P. Nikolaev, I.A. Ozheredov, M. V. Chukalina, A. P. Shkurinov. A.P.Suppression algorithm for the orthotropic artifacts in images registered in X-ray and terahertz band. Information Processes. 19(2), 2019, pp. 200–207 (In Russian).

[11] T. Sanders, M. Prange, C. Akatay, P. Binev. Physically motivated global alignment method for electron tomography. Adv Struct Chem Imag 1, 4 (2015) doi:10.1186/s40679-015-0005-7.

[12] K. Jun, S. Yoon. Alignment Solution for CT Image Reconstruction using Fixed Point and Virtual Rotation Axis. Scientific Reports, 2018, 7:41218, DOI: 10.1038/srep41218.

[13] A. Buzmakov, M. Chukalina, D. Nikolaev, V. Gulimova, S. Saveliev, E. Tereschenko, A. Seregin, R. Senin, D. Zolotov, V. Prun, G. Shaefer and V. Asadchikov. Monochromatic computed microtomography using laboratory and synchrotron sources and X-ray fluorescence analysis for comprehensive analysis of structural changes in bones. Journal of Applied Crystallography 48(3), 2015, pp 693-701.

[14] Marina Chukalina, Dmitry Nikolaev, Anastasia Ingacheva, Alexey Buzmakov, Ivan Yakimchuk, and Victor Asadchikov "To image analysis in computed tomography", Proc. SPIE 10341, Ninth International Conference on Machine Vision (ICMV 2016), 103411B (17 March 2017); https://doi.org/10.1117/12.2268616

[15] A.I. Ingacheva, A.V. Sheshkus, T.S. Chernov, E.E. Limonova, V.V. Arlazarov. "X-ray computer tomograph is a new tool for recognition". Trudy ISA RAN, 2018, 68(S1), p.90-99.DOI 10.14357/20790279180510

[16] I. A. Kunina, S. A. Gladilin, D. P. Nikolaev, "Blind radial distortion compensation in a single image using fast Hough transform", Computer optics, 2016, 40(3), p. 395-403. DOI 10.18287/2412-6179-2016-40-3-395-403

[17] Denis Zolotov, Alexey Buzmakov, Maxim Grigoriev and Igor Schelokov. Dual-energy crystal-analyzer scheme for spectral tomography // Journal of Applied Crystallography. 2020. V.53. pp. 781-788. DOI: 10.1107/S1600576720005439